Performance of Uncoded Space-Time Labelling Diversity over Dual-Correlated Rayleigh-Fading Channels

Sulaiman Saleem Patel[#1], Tahmid Quazi[#2], Hongjun Xu[#3]

[#]*School of Electrical, Electronic and Computer Engineering, University of Kwa-Zulu Natal, South Africa*

[1]sulaiman.s.patel@gmail.com

[2]quazit@ukzn.ac.za

[3]xuh@ukzn.ac.za

Abstract—**Uncoded Space-Time Labelling Diversity (USTLD) is a recent technique to improve error performance in multiple-input, multiple-output (MIMO) systems. Standard MIMO systems assume that channels between transmit and receive antennas are independent and identically distributed (i.i.d.), and thus, uncorrelated. This assumption is also made in previous works on USTLD. However, in practice, if antennas are spaced closer than half a transmission wavelength to each other, channels become correlated. This motivates the study in this paper of the performance of USTLD under correlated channel conditions. An analytical expression for the upper bound of the average bit error rate (BER) in the presence of correlated fading is derived. This expression is validated using results from Monte Carlo simulations, which show a tight fit in the high signal-to-noise ratio (SNR) region. Results presented confirm that channel correlation adversely affects the BER of USTLD for both 16QAM and 64QAM. Interestingly, results also indicate that USTLD is more sensitive to channel correlation than comparable standard MIMO schemes.**

***Keywords*— correlated Rayleigh fading, labelling diversity, uncoded system, USTLD, MIMO**

I. INTRODUCTION

Wireless communication systems suffer impaired performance due to the existence of multipath fading [1]. The effects of fading may be combatted by incorporating diversity into the system. Uncoded Space-Time Labelling Diversity (USTLD) [2] is a recent scheme that provides three levels of diversity: labelling diversity, time diversity and antenna diversity. To achieve labelling diversity, USTLD exploits the mapping of binary data to different constellations through the use of two different mappers. Antenna diversity is achieved by adopting a multiple-input, multiple-output (MIMO) system model. The inclusion of multiple antennas at both the transmitter and receiver generates more signal paths, increasing the likelihood of correct detection [1], [3]. The original work on USTLD describes a MIMO system of two transmit antennas and any arbitrary N_r receive antennas. To achieve time diversity and protect against burst errors, symbols representing the same binary data are transmitted in separate time slots. In each time slot, symbols are selected from constellations with different binary mappings. The design and selection of mappers aims to maximise the summed Euclidean Distance (ED) between symbol pairs in each constellation. Stated differently, adjacent symbols in a given mapping are spaced further apart in subsequent mappings. By following this approach, detection is done based on symbol pairs, instead of individual symbols. For an MQAM or MPSK system, there are only M valid symbol pairs out of the M^2 possible pairs. Thus, diversity is achieved in a manner similar to conventional error correction codes [4], even though USTLD is an uncoded system.

The MIMO structure of USTLD is important when analysing its BER performance. In conventional analysis of antenna diversity systems [3], it is assumed that signal paths are statistically independent of each other i.e. the channels are uncorrelated. However, this assumption is invalid if the spacing between antennas in less than half the transmitted wavelength (λ) [5]. Due to the inversely proportional relationship between frequency and wavelength [5], the required spacing between antennas to prevent correlation at higher transmission frequencies becomes unfeasibly small. However, the use of higher transmission frequencies is desirable as it results in greater throughput per second [3]. When physical conditions are such that antennas are spaced closer than $\frac{\lambda}{2}$ from each other, the signal paths between them become correlated, and the conventional models of system analysis no longer apply.

The first case study [6] of the effect of correlation on multiple antenna systems considered the single-input dual-correlated channel (i.e. the case of one transmit antenna and two receive antennas). In [6], it is shown that an orthogonal transformation may be applied to identical dual-correlated channels to generate equivalent uncorrelated, non-identical channels for statistical analysis. In [7], the more general case of N_r receiver antennas is considered. Instead of using orthogonal transformations, this work indicates the design of a decorrelating and signal splitting eigenfilter based on the correlation matrix between antennas. The result of using the eigenfilter approach allows the correlated channels to be analysed as uncorrelated, eigenvalue-weighted independent channels. While both [6] and [7] constrain their analysis to SIMO systems, other works [8]-[10] provide the mathematical framework for correlated MIMO systems – which considers correlation between any N_t transmit antennas and N_r receive antennas. However, in [11], the validity of the Kronecker model, a fundamental model applied in [8]-[10] to account for correlation, is questioned. According to the findings of [11], the Kronecker model may not be valid for antenna arrays larger than a 2×2 system when the correlation between channels is high.

In the original work on USTLD [2], the $2\times N_r$ MIMO system model assumes uncorrelated channels. In this work, the performance of USTLD in correlated channels is studied. To ensure the validity of the MIMO Kronecker correlation model used, as per [11], this study is constrained to the case of a 2×2 system.

The remainder of this paper is structured as follows: in Section II describes the system model used, including the selection of USTLD mappers. In Section III, an analytical expression is derived for the upper bound of the average bit error probability (ABEP) of USTLD under correlated conditions. Section IV presents the results of Monte Carlo simulations investigating USTLD in correlated and uncorrelated channels. Finally, Section V presents the conclusions which may be drawn from the results.

For consistent notation, this paper denotes vectors in boldface, lowercase type. Scalars are represented in italicised lowercase, and matrices are represented by italicised uppercase. The only exceptions to this notation are variables N_r and N_t which are scalars.

II. System Model

A. Uncorrelated USTLD Transmission Model

The system model for this study considers a 2×2 MIMO system and the transmission of data over two time slots. The 2×1 received vector, **r**, during the k^{th} time slot is given by

$$\mathbf{r}_{\mathrm{k}} = \sqrt{\frac{\gamma}{2}}\left(\mathbf{h}_{1,k}x_{1,k} + \mathbf{h}_{2,k}x_{2,k}\right) + \mathbf{n}_k \tag{1}$$

As necessitated by USTLD, transmitted symbols x_1 and x_2 in (1) are selected from different mappers in each time slot. During time slot $k = 1$, a Gray-coded mapper, denoted Ω_1, is used [2]. During time slot $k = 2$, a secondary mapper, Ω_2, is selected. 16QAM and 64QAM modulation schemes are investigated. For the second mapper, this system chooses the 16QAM mapping proposed by [12], illustrated in Fig. 1, which is found to be optimal according to [12] and [2]. In [12], the optimal mapping design technique used is only feasible for up to 16-ary constellation sizes. Therefore, the simple but effective mapping procedure proposed in [2] is used in constructing Ω_2 for 64QAM. The mapper is constructed by interchanging diagonal elements in diagonally opposite quadrants, as proposed in [2]. That is, diagonal elements in quadrant 1 are interchanged with corresponding diagonal elements in quadrant 3; and similarly for quadrants 2 and 4. All constellations are power-normalised such that $E\{|x|^2\} = 1$, where $E\{\cdot\}$ is the statistical expectation operator.

Figure 1: 16QAM Constellation Mappings (Key: Ω_1/Ω_2)

γ is the total signal-to-noise ratio of the transmission, distributed equally between the two transmit antennas. 2×1 vector **n** represents additive white Gaussian noise (AWGN) which follows a complex normal distribution with zero mean and variance $\sigma_n{}^2 = \frac{N_0}{2}$ per dimension. 2×1 vectors $\mathbf{h}_1$ and $\mathbf{h}_2$ represent the fast-fading channels due to respective transmit antennas. The fading follows a Rayleigh amplitude distribution of zero mean and unit variance, the probability density function of which is $f_{Rayleigh}(\alpha) = \frac{\alpha}{2\pi}e^{-\frac{1}{2}\alpha^2}$, where α is the fading amplitude. Both the fading channels and AWGN noise have uniform phase distribution.

B. Correlated Channel Model

The correlation between the i^{th} and j^{th} elements of **h** is defined according to [5] as

$$\rho_{i,j} = \frac{E\{h_i\overline{h_j}\}}{\sqrt{\sigma_i^2\sigma_j^2}} \tag{2}$$

where the overbar $\overline{(\cdot)}$ denotes a complex conjugate and σ^2 is the variance of the fading branch. From (2) it is also clear that $\rho_{i,j} = \rho_{j,i}$. The correlation matrix for a 2×2 system may then be defined as

$$C_{2\times 2} = \begin{bmatrix} 1 & \rho \\ \rho & 1 \end{bmatrix} \tag{3}$$

In [5] and [7], it is shown that the correlation between receiver antennas may be expressed as a function of the spacing between them, $\mu_{i,j}$, as

$$\rho_{i,j} = J_0\left(\frac{2\pi\mu_{i,j}}{\lambda}\right) \tag{4}$$

Here, λ is the wavelength of transmission and $J_0(\cdot)$ is the zeroth order Bessel function of the first kind. It is assumed in (4) that the transmitter and receiver are sufficiently far apart that any phase difference in the received signal due to spacing between transmit antennas is negligible. As such, the spacing between transmit antennas is not considered in (4).

C. Detection

Maximum likelihood detection (MLD) in USTLD requires that received symbol vectors from both time slots are considered simultaneously. Unlike conventional MIMO detection, MLD for labelling diversity is concerned with joint detection using corresponding symbols from both mappers. As such, the output of the ML detector is two sets of symbol pairs, $\tilde{\mathbf{x}}_1$ and $\tilde{\mathbf{x}}_2$. Detected data corresponds to the label associated with each of these pairs. The ML detection metric based on (1) is

$$\tilde{\mathbf{x}}_1, \tilde{\mathbf{x}}_2 = \arg\min_{\hat{\mathbf{x}}_k \in \Omega_k} \sum_{k=1}^{2} \left\| \mathbf{r}_k - \sqrt{\frac{\gamma}{2}} H_k \hat{\mathbf{x}}_k \right\|^2 \tag{5}$$

where $H_k = [\mathbf{h}_{1,k} \quad \mathbf{h}_{1,k}]$ and $\hat{\mathbf{x}}_k = \begin{bmatrix} \hat{x}_{1,k} \\ \hat{x}_{2,k} \end{bmatrix}$ and $\|\cdot\|^2$ denotes a vector norm**.** Perfect channel state information is assumed to be available at the receiver to perform coherent MLD.

III. Performance Analysis

A. Uncorrelated USTLD in Rayleigh Fading Channels

An approach to analysing the average bit error probability (ABEP) in uncorrelated channels is given in [2]. This analysis applies to both fast-fading and quasi-static Rayleigh fading conditions.

An important assumption at the start of this analysis is that at high SNR, one of the two transmitted symbol pairs is correctly detected. Given this, the upper bound of the ABEP for USTLD is defined as [2]

$$P_B(\gamma) \leq \frac{1}{M \log_2 M} \sum_{i=1}^{M} \sum_{j \neq i}^{M} \delta(i,j) P(X \to \tilde{X}) \quad (6)$$

where $\delta(i,j)$ are the number of bit errors between the labels i and j and $P(X \to \tilde{X})$ is the pairwise error probability of an erroneous detection of vector $X = \begin{bmatrix} x_{1,1} & x_{2,1} \\ x_{1,2} & x_{2,2} \end{bmatrix}$ to estimated vector $\tilde{X} = \begin{bmatrix} \tilde{x}_{1,1} & \tilde{x}_{2,1} \\ \tilde{x}_{1,2} & \tilde{x}_{2,2} \end{bmatrix}$.

The number of bit errors may be calculated as,

$$\delta(i,j) = \sum_{k=1}^{\log_2 M} b_k^i \oplus b_k^j \quad (7)$$

where b_k^i is the k^{th} bit of i, b_k^j is the k^{th} bit of j and $\oplus$ is the binary exclusive-or (xor) operator. At this point, a distinction between the number of bit errors $\delta(i,j)$ and the Euclidean distance $d_k(i,j)$ is made.

$$d_k(i,j) = \left|x_i - x_j\right|^2;\ x_i, x_j \in \Omega_k \quad (8)$$

Given the assumption that only one symbol pair is incorrect, the conditional PEP may be expressed according to (9). This may be simplified in terms of the Gaussian Q-function and two central chi-squared random variables ϕ_1 and ϕ_2 as

$$P(X \to \tilde{X}\ |H_1, H_2) = Q\left(\sqrt{\phi_1 + \phi_2}\right) \quad (10)$$

The chi-squared random variables have $2N_r$ degrees of freedom and may be defined as

$$\phi_k = \sum_{n=1}^{2N_r} \alpha_{k_n}^2 \quad (11)$$

The random variable $\alpha_{k_n}^2$ follows a normal distribution according to $\alpha_{k_n} \sim N\left(0, \frac{\gamma}{8} d_k\right)$. It then follows that the moment generating function (MGF) for random variable ϕ_k under the assumption of N_r i.i.d. channels is given by

$$M_k(s) = \int_0^\infty f_{\phi_k}(\alpha_k) e^{-s\alpha_k} d\alpha_k = \left(1 + \frac{\gamma}{4} d_k s\right)^{-N_r} \quad (12)$$

In (12), $f_{\phi_k}(\alpha_k)$ is the probability density function (PDF) of the chi-squared random variable given by

$$f_{\phi_k}(\alpha_k) = \frac{1}{\left(\frac{\gamma}{4} d_k\right)^{N_r} (N_r - 1)!} e^{-\frac{4\alpha_k}{\gamma d_k}} \quad (13)$$

Integrating the conditional PEP over the PDFs for ϕ_1 and ϕ_2 as shown in (14) and applying the trapezoidal approximation to Craig's representation of the Gaussian Q-function (15), it is found that the PEP in is given by (16). In order to simplify analysis in Subsection B, where correlation between channels is considered, the overall ABEP is expressed in terms of MGF functions. The overall ABEP in uncorrelated Rayleigh fading channels, given in (17), is then obtained by substituting (7) and (16) in (6).

B. Correlated Channel Analysis

According to [8]-[9], the correlated channel matrix H may be expressed in terms of an uncorrelated matrix H_{uc} by the Kronecker model,

$$H = C_r^{\frac{1}{2}} H_{uc} \left(C_t^{\frac{1}{2}}\right)^T \quad (18)$$

where C_r and C_t are the correlation matrices due to the transmitter antennas and receiver antennas respectively and $(\cdot)^T$ denotes the matrix transpose operator. It is shown in [7]-[10] that the effect of correlation may be taken into account by considering the eigenvalues of the correlation matrices. In other words, the correlated channels may be analysed as statistically independent, eigenvalue-weighted uncorrelated channels.

The eigenvalue decomposition (EVD) [10], [12] of the correlation matrix into a matrix of unitary, orthogonal eigenvectors, Z, and a diagonal matrix of positive eigenvalues, Λ, is defined as

$$C_r = Z_r^H \Lambda_r Z_r \quad (19)$$

$$C_t = Z_t^H \Lambda_t Z_t \quad (20)$$

where subscript r and t are the indices for the receive and transmit antennas respectively. The notation $(\cdot)^H$ above refers to the Hermitian (conjugate transpose) operator. The individual entries of Λ_r are referred to as λ^r, and similarly the individual entries of Λ_t are referred to as λ^t. As per [8], the effect of fading on $N_t N_r$ correlated channels in a MIMO system may be modelled by the MGFs of non-indentical, uncorrelated channels as

$$M_c(s) = \prod_{i=1}^{N_t} \prod_{j=1}^{N_r} M_{uc}(s \lambda_i^t \lambda_j^r) \quad (21)$$

$$P(X \to \tilde{X}\ |H_1, H_2) = P\left(\left\|\mathbf{r}_1 - \sqrt{\frac{\gamma}{2}} H_1 \tilde{\mathbf{x}}_1\right\|^2 + \left\|\mathbf{r}_2 - \sqrt{\frac{\gamma}{2}} H_2 \tilde{\mathbf{x}}_2\right\|^2 < \left\|\mathbf{r}_1 - \sqrt{\frac{\gamma}{2}} H_1 \mathbf{x}_1\right\|^2 + \left\|\mathbf{r}_2 - \sqrt{\frac{\gamma}{2}} H_2 \mathbf{x}_2\right\|^2\right) \quad (9)$$

$$P(X \to \tilde{X}) = \int_0^\infty \int_0^\infty P(X \to \tilde{X}\ |H_1, H_2) f_{\phi_1}(\alpha_1) f_{\phi_2}(\alpha_2) d\alpha_1 d\alpha_2 \quad (14)$$

$$Q(x) = \frac{1}{\pi} \int_0^{\frac{\pi}{2}} e^{-\left(\frac{x^2}{2} \operatorname{cosec}^2 y\right)} dy \cong \frac{1}{2n}\left(\frac{1}{2} e^{-\frac{1}{2}x^2} + \sum_{l=1}^{n-1} e^{-\left(\frac{x^2}{2} \operatorname{cosec}^2\left(\frac{l\pi}{2n}\right)\right)}\right) \quad (15)$$

$$P(X \to \tilde{X}) = \frac{1}{2n}\left[\frac{1}{2} \prod_{l=1}^{2} M_l\left(\frac{1}{2}\right) + \sum_{m=1}^{n-1} \prod_{l=1}^{2} M_l\left(\frac{1}{2} \operatorname{cosec}^2\left(\frac{m\pi}{2n}\right)\right)\right] \quad (16)$$

$$P_B(\gamma) \leq \frac{1}{2nM \log_2 M} \sum_{i=1}^{M} \sum_{j \neq i}^{M} \left(\sum_{k=1}^{\log_2 M} b_k^i \oplus b_k^j\right)\left[\frac{1}{2} \prod_{l=1}^{2} M_l\left(\frac{1}{2}\right) + \sum_{m=1}^{n-1} \prod_{l=1}^{2} M_l\left(\frac{1}{2} \operatorname{cosec}^2\left(\frac{m\pi}{2n}\right)\right)\right] \quad (17)$$

For the system considered in this work, it is assumed that sufficient physical space is available at the transmitter that transmit antennas are uncorrelated. This is reasonable in cases such as the base stations in a mobile communication system. Uncorrelated transmit antennas yields an identity matrix for C_t, which has unit eigenvalues.

For the special case of 2 receive antennas, the eigenvalues may be given as

$$\lambda_1^r = 1 + \rho \tag{22}$$

$$\lambda_2^r = 1 - \rho \tag{23}$$

(22) and (23) are the same channel weights obtained by the orthogonal transform approach adopted in [6].

The MGF for USTLD under dual-correlated receiver conditions may be obtained by substituting (22) and (23) in Equation (21), producing (24).

Extending (17) with the expression from (23) yields (24) – the upper bound of the ABEP for a USTLD system subject to Rayleigh fading that is dual-correlated at the receiver. Note that the MGFs in (24) represent non-identical, independent channels, so when substituting (12) in (24), $N_r = 1$.

IV. Simulation Results and Discussion

Monte Carlo simulations were conducted to investigate the performance of 2×2 USTLD systems in the presence of correlated Rayleigh fading. In the simulation model, the approach in [13] is used to ensure the generation of adequately correlated random variables to simulate the channels. To ensure a clear distinction between correlated and uncorrelated results, the case of receive antennas spaced very close together, such that $\mu_{1,2} = 0.1\lambda$, is considered. From (4), this yields a correlation coefficient of

$$\rho_{1,2} = J_0\left(\frac{2\pi(0.1\lambda)}{\lambda}\right) = 0.904 \tag{26}$$

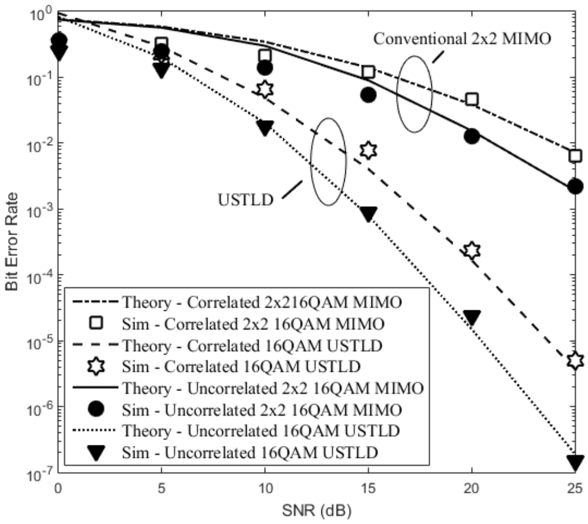

Figure 2: Performance of 16QAM and 16QAM USTLD in Dual-Correlated Channels ($\mu_{1,2} = 0.1\lambda$)

The first set of simulation results presented in Figs. 2 and 3 show that the theoretical upper bound of the ABEP converges to match simulated results at high SNR. In Fig. 2, the performance of a conventional 2×2 16QAM MIMO system and 16QAM USTLD are compared for the cases of uncorrelated and correlated channels. Likewise, Fig. 3 shows the results of the same comparison for a 2×2 64QAM MIMO system and 64QAM USTLD.

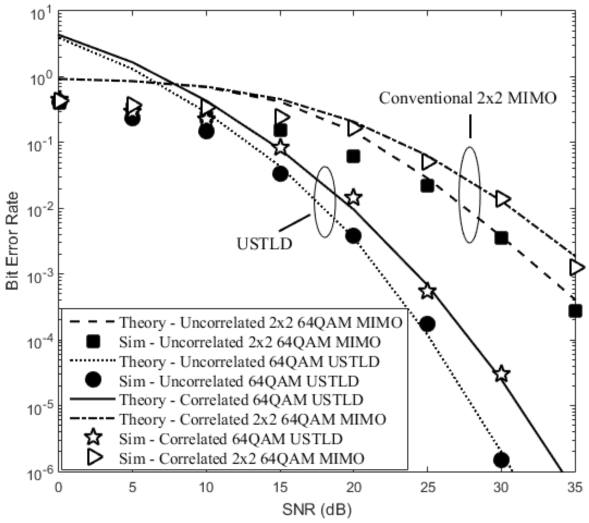

Figure 3: Performance of 64QAM and 64QAM USTLD in Dual-Correlated Channels ($\mu_{1,2} = 0.1\lambda$)

From Figs. 2-3, it is evident that even under highly correlated conditions, USTLD still provides significant diversity gain over conventional 2×2 MIMO systems. However, from the dB gap between correlated and uncorrelated curves, it appears that USTLD is more sensitive to channel correlation than standard MIMO schemes. This is observed intuitively by noting that the dB gap between correlated and uncorrelated USTLD is wider than the dB gap between the correlated and uncorrelated conventional 2×2 MIMO systems.

In order to further investigate this observation, the effect of varying correlation on BER is examined in Figs. 4 and 5. In Fig. 4, 16QAM USTLD is compared against Gray-coded 2×2 16QAM MIMO system, and against Gray-coded 2×2 4QAM MIMO system. A 2×2 Gray-coded 4QAM may be considered comparable as it offers the same data rate (4 bits/s/Hz) as 16QAM USTLD. Similarly, in Fig. 5, 64QAM USTLD is compared against a 2×2 64QAM MIMO system and a 3×2 4QAM MIMO system. The 3×2 4QAM MIMO system is preferred over a 2×2 8QAM MIMO system so that square MQAM analysis may still be used. Both of these schemes offer the same data rate (6 bits/s/Hz) as 64QAM USTLD.

$$M_c(s) = \prod_{i=1}^{2} M_{uc}(s\lambda_i^r) = M_{uc}\big(s(1+\rho)\big)\, M_{uc}\big(s(1-\rho)\big) \tag{24}$$

$$P_B(\gamma) \le \frac{1}{2nM\log_2 M}\sum_{i=1}^{M}\sum_{j\neq i}^{M}\left(\sum_{k=1}^{\log_2 M} b_k^i \oplus b_k^j\right)\left[\frac{1}{2}\prod_{l=1}^{2} M_l\left(\frac{1}{2}\lambda_l^r\right) + \sum_{m=1}^{n-1}\prod_{l=1}^{2} M_l\left(\frac{1}{2}\lambda_l^r \operatorname{cosec}^2\left(\frac{m\pi}{2n}\right)\right)\right] \tag{25}$$

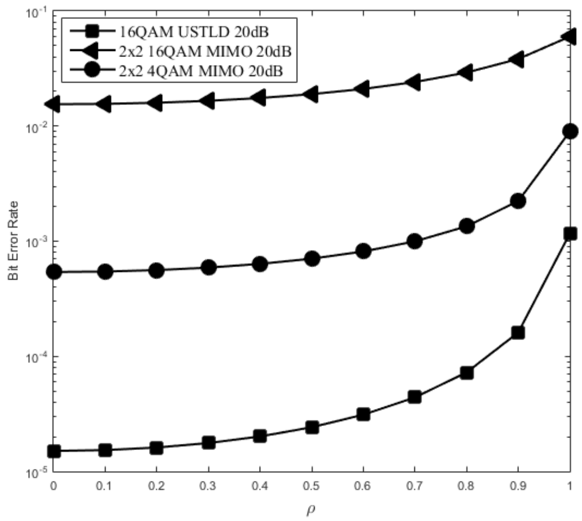

Figure 4: Effect of Channel Correlation on BER for 16QAM USTLD

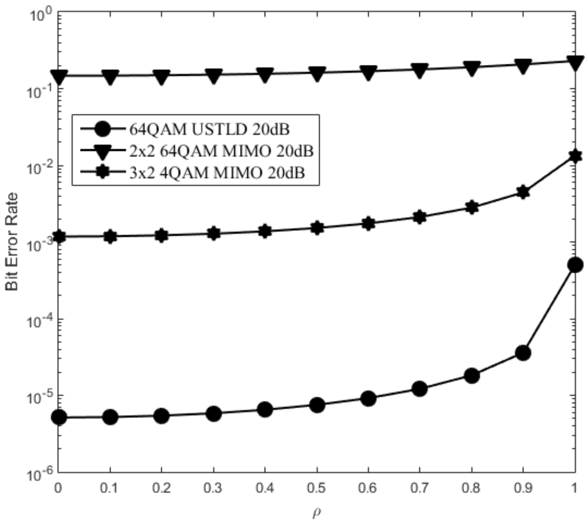

Figure 5: Effect of Channel Correlation on BER for 64QAM USTLD

The slope of the curves in Figs. 4 and 5 indicate the rate at which system performance deteriorates as channel correlation increases. It is clear, however, that in both cases, the USTLD curves show the steepest ascent as correlation coefficient increases. Thus, these results indicate that USTLD is more sensitive to channel correlation than comparable standard MIMO schemes.

V. CONCLUSION

In this work, the impact of correlated channels on USTLD systems is investigated. The study is restricted to a 2×2 system. An expression is derived for the upper bound of the ABEP, which is shown to converge to simulation results in the high SNR region. Results indicate that USTLD is still capable of providing diversity gain when channels are highly correlated. However, compared to standard MIMO systems, the performance of USTLD deteriorates faster as channel correlation increases. Future work may include investigating the performance of USTLD in the presence of both transmit antenna correlation and receive antenna correlation.

ACKNOWLEDGMENT

The primary author would like to firstly acknowledge God Almighty, without whom no achievements are possible. Thereafter, acknowledgement goes to Dr Quazi and Prof Xu, for all their guidance and patience, and to his family, for continuous support at all times.

REFERENCES

[1] M. K. Simon and M. S. Alouini, *Digital Communication over Fading Channels*, 2nd ed., J. Wiley & Sons, 2005.

[2] H. Xu, K. Govindasamy and N. Pillay, “Uncoded Space-Time Labeling Diversity,” *IEEE Communications Letters*, vol. 20, no. 8, pp. 1511-1514, Aug. 2016.

[3] A. Goldsmith, *Wireless Communications*, Cambridge University Press 2005.

[4] S. Haykin and M. Moher, *Communication Systems*, 5th ed., J. Wiley & Sons, 2010.

[5] G. L. Stüber, *Principles of Mobile Communication*, 2nd ed., Kluwer Academic Publishers, 2002.

[6] L. Fang, G. Bi and A. C. Kot, “New Method of Performance Analysis for Diversity Reception with Correlated Rayleigh-fading Signals”, *IEEE Transactions on Vehicular Technology*, vol. 49, no. 5, pp. 1807-1812, Sept. 2000.

[7] P. O. Akuon and H. Xu, “Optimal error analysis of receive diversity schemes on arbitrarily correlated Rayleigh fading channels”, *IET Communications*, vol. 10, no. 7, pp. 854-861, Jan. 2016.

[8] A. Hedayat, H. Shah and A. Nosratinia, “Analysis of Space–Time Coding in Correlated Fading Channels”, *IEEE Transactions on Wireless Communications*, vol. 4, no. 6, pp. 2882-2891, Nov. 2005.

[9] B. Kumbhani, V. K. Mohandas, R. P. Singh, S. Kabra and R.S. Kshetrimayum, “Analysis of Space-Time Block Coded Spatial Modulation in Correlated Rayleigh and Rician Fading Channels”, in *2015 IEEE Int. Conf. Digital Signal Processing*, 2015, pp. 516-520.

[10] A. Saad, M. Ismail and N. Misran, “Correlated MIMO Rayleigh Channels: Eigenmodes and Capacity Analyses”, *Int. Journal of Computer Science and Network Security*, vol. 8, no. 12, pp. 75-81, Dec. 2008.

[11] C. Oestges, “Validity of the Kronecker Model for MIMO Correlated Channels”, in *IEEE 63rd Vehicular Technology Conference 2006-Spring*, 2006, pp. 2818-2822.

[12] H. Samra, Z. Ding and P. M. Hahn, “Symbol Mapping Diversity Design for Multiple Packet Transmissions”, *IEEE Transactions on Communications*, vol. 53, no. 5, pp. 810-817, May 2005.

[13] L. Fang, G. Bi and H. Fu, “Generation of Two Correlated Rayleigh Fading Signals with Arbitrary Powers”, *Journal of Communications and Networks*, vol. 1, no. 4, pp. 266-268, Dec. 1999.

Sulaiman Saleem Patel is a MScEng student at the University of Kwa-Zulu Natal. He completed his BScEng in Electronic Engineering Summa Cum Laude in 2015. Sulaiman is currently part of the UKZN Armscor research group and Vice-President of the IEEE-HKN Student Chapter, Mu Eta, at UKZN.